A Comparative Study Between Light Extinction and Direct Sampling Methods for Measuring Volume Fractions of Twin-Hole Sprays Using Tomographic Reconstruction

Choong Hoon Lee*

Department of Automotive Engineering, Seoul National University of Technology, Seoul 139-743, Korea

The spatially resolved spray volume fractions from both line-of-sight data of direct measuring cells and a laser diffraction particle analyzer (LDPA) are tomographically reconstructed by the Convolution Fourier transformation, respectively. Asymmetric sprays generated from a twin-hole injector are tested with 12 equiangular projections of measurements. For each projection angle, a line-of-sight integrated injection rate was measured using a direct sampling method and also a liquid volume fraction from a set of line-of-sight Fraunhofer diffraction measurements was measured using a light extinction method. Interpolated data between the projection angles effectively increase the number of projections, significantly enhancing the signal-to-noise level in the reconstructed data. The reconstructed volume fractions from the direct sampling cells were used as reference data for evaluating the accuracy of the volume fractions from the LDPA.

Key Words: Light Extinction, LDPA, Direct Sampling, Tomographic Reconstruction

1. Introduction

A laser diffraction particle analyzer provides line-of-sight integrated volume fractions. However, a beam scattering length must be provided in order to calculate the line-of-sight integrated volume fractions. A LDPA mannfacturer (Malvern Instrument, 1991) provides a standard beam scattering vessel that defines a beam scattering length. This process in calculating volume fractions with the LDPA is inconvenient and has limitations that cannot provide spatially resolved volume fractions. On the other hand, the spatially resolved spray volume fractions can be obtained from tomographic reconstruction of line-of-sight Fraunhofer diffraction measurements, which is independent of the beam scattering length. The accuracy of the spatially resolved volume fractions from the LDPA's data could be evaluated by comparison with that from the direct sampling cells for the same experimental conditions. To author's knowledge, the estimation about the accuracy of the spatially resolved volume fractions from the LDPA's data has not been previously reported in the existing literatures.

The tomographic reconstruction approach, which is one of mathematical inversion problems from a multi-directional exploration of the field, has been widely applied to medicine (Cormack, 1963, 1974; Gordon et al., 1975), optics (Rowley, 1969; Cha and Sun, 1990; Cha and Cha, 1996) and heat transfer (Sweeny and Vest, 1973; Slepicka and Cha, 1997). In general, the algorithms employed for reconstruction fall into three categories: Fourier transforms, linear superposition and algebraic reconstruction techniques (ART). When a rapid detailed mapping is required, convolution methods seem best, whereas algebraic reconstruction may be most effective

* **E-mail** : chlee5@snut.ac.kr
TEL : +82-2-970-6393; **FAX** : +82-2-979-7032
Department of Automotive Engineering, Seoul National University of Technology, Seoul 139-743, Korea.
(Manuscript **Received** May 15, 2003; **Revised** August 26, 2003)

when only a limited number of angles are available (Eckbreath, 1987).

The reconstruction for an axisymmetric spray requires measurements at only a single projection angle and the relatively simple Abel transformation of the projected data can determine radially resolved data (Dodge et al., 1987; Yule et al., 1981; Zhu et al., 1987; Jeong and Lee, 1992). Asymmetric sprays are often encountered in diverse industrial systems such as multiple-hole diesel injector sprays and elliptic cross-section cooling sprays for sheet metal rolling process. Reconstruction of asymmetric sprays envisions more complicated features than that of symmetric sprays in two fold: 1) a number of projections at different angles are needed to ensure the accuracy and stability of the inverse transformation calculations, usually the more projections give the better reconstruction, and 2) a more rigorous deconvolution scheme is required to solve an indeterministic conversion problem of multiangular scannings where the number of unknowns does not match with the number of the constraint equations. Tomographic reconstruction of asymmetric sprays has been previously studied by Lee and Chung (1997), and Yang et al.(1999).

The present work examines asymmetric sprays generated from a twin-hole air shroud injector that simulates spark ignition engine sprays. Multiangular scanning of a Fraunhofer diffraction measurement probe (Malvern 2600-D system) and direct sampling cells provides line-of-sight integrated data that are tomographically reconstructed to determine cross-sectionally distributing spray parameters. The reconstruction has been carried out by using the convolution Fourier transforms that are based on Fourier slice theorem (Kak and Slaney, 1988; Santro et al, 1981; Goulard and Emmerman, 1980). An improvement on the conventional convolution Fourier transformation has been made to effectively double or triple the number of projections by interpolating between two adjacent projections and creating interpolated data sets in between.

The spatially resolved volume fraction is tomographically reconstructed from the direct sampling cell data to estimate the accuracy of that from the LDPA's line-of-sight data. The conversion coefficient C_f between the LDPA's and the direct sampling cell's volume fractions was obtained from the comparative study.

2. Experiment

2.1 LDPA experiment

Figure 1 shows the schematic diagram of experimental apparatus for the LDPA masurement, which consists of a tested twin-hole air shroud nozzle designed for a gasoline injector (Bosch Inc.), a positioning system for the nozzle assembly, and a diffraction measurement system. The two orifices constitute an injection angle of 22° and each circular orifice of diameter 0.3 mm develops a spray with approximately 10° of spray divergence. The twin-hole air shroud injector is developed to reduce hydrocarbon emissions from gasoline engines by promoting finer atomization through the interaction of shroud air and fuel jet, thereby achieving enhanced evaporation of fuel.

Water is used as the atomizing liquid and is injected into atmospheric at a fixed flow rate of 4 ml/s with a constant injection pressure of 0.44 MPa in gauge. The shroud air pressure maintains at 0.03 MPa in gauge.

The nozzle assembly is fixed at a scanning angle and horizontally moves at a 2 mm interval for 51 measurement points. After the measurements for the fixed angle the same processes are repeated rotating the nozzle assembly at a 15° interval to allow measurements at 12 different

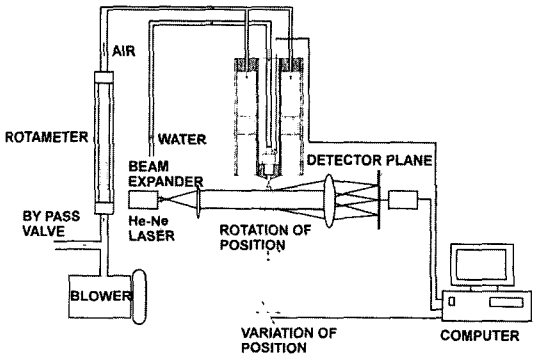

Fig. 1 Schematic of LDPA experimental setup

equiangular projections. It took approximately 2 hours for obtaining the whole measured data set for 12 different equiangular projections. The averaged value from five realizations of each 500 internal sweep at each measurement point is recorded to form the basic data to be reconstructed. For analyzing laser diffraction signals in the Malvern system, a drop size distribution function shold be assumed. Here, we have adopted the two-parameter model of Rosin-Rammler distribution. The measurements are conducted at the axial location $z=90$ mm downstream from the nozzle exit. This position was selected based on the obscuration in the laser measurement and on the experimental convenience.

2.2 Experiment using direct sampling cells

The sampling cells are made of an aluminum block having the dimensions of 210 mm×100 mm×55 mm. By the electro-discharge wire-cutting machining, a total of 60 cells were made in the block. Each cell is 3 mm wide, 100 mm long and 55 mm deep and is separated by a 0.5 mm thickness wall as schematically shown in Fig. 2. The sides of the sampling cells are covered with plexiglass plates and small drain holes were made at the bottom plate of each cell. Flow distributions are analyzed by placing the sampling cells with a set of multi-angular scanning angles.

For a comparative study between the LDPA and the direct sampling cells, experimental conditions for spray injections are chosen to be the same as those of the LPDA measurement described previously. Each projection samples sprays' drops directly with 35 measurement cells that are separated horizontally at a 3.5 mm interval. Flow distribution collected in the sampling cells is calculated by dividing the sampled water volume in each cell by the sampling time.

2.3 Visualization

Figure 3 shows instantaneous spray images with and without shroud air. A Nd-YAG laser sheet beam is used as a light source. With no shroud air, two nearly separate sprays (Fig. 3(a)) develop along the inclined injection angles. With the shroud air, small droplets are observed in the region between the two primary sprays (Fig. 3 (b)).

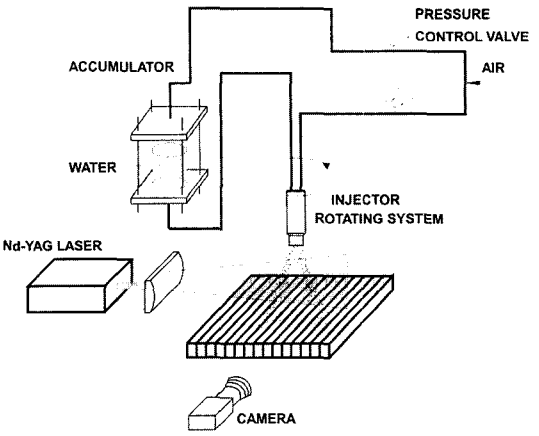

Fig. 2 Experimental setup using a direct sampling cells

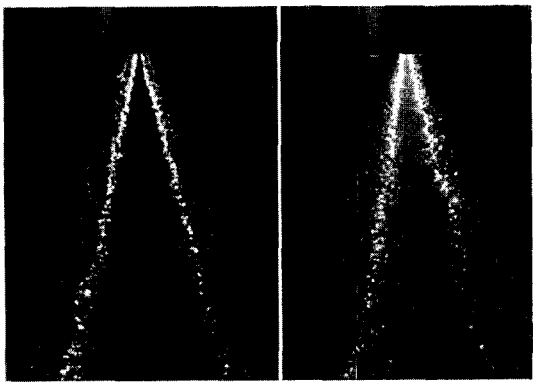

(a) (b)

Fig. 3 Photographs showing spray structure from twin hole injector with injection pressure of 0.44 MPa in gage, (a) without and (b) with air shroud (air pressure 0.03 MPa in gage)

3. Tomographic Reconstruction

The direct sampling cells provide line-of-sight integrated data for the spray sampling rate $f(r, \theta)$ along each projection plane at θ (Fig. 4), which is a conserved quantity in the line-of-sight integration. Tomographic reconstruction finds the cross-sectional distribution of $f(x, y)$, which is readily determined from the conserved quantity.

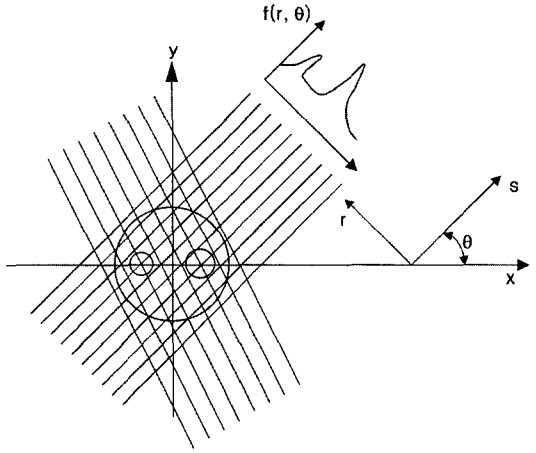

Fig. 4 Schematics showing multi-angular scanning measurement and coordinates system

The measured projection data and the cross-sectional data are related by a line-of-sight integral:

$$f(r,\ \theta)=\frac{1}{L}\int_{-\infty}^{\infty}f(x,\ y)\,ds \tag{1}$$

where L is the width of direct sampling cells.

The Fourier transformation of $f(r,\ \theta)$ is

$$f(\omega,\ \theta)=\int_{-\infty}^{\infty}e^{-i\omega r}f(r,\ \theta)\,dr \tag{2}$$

On the other hand, two-dimensional Fourier transformation of $f(x,\ y)$ yields

$$F_V(\omega,\ \theta)=\int_{-\infty}^{\infty}\int_{-\infty}^{\infty}f(x,\ y)\exp[-i\omega(x\cos\theta+y\sin\theta)]\,dxdy \tag{3}$$

The central slice theorem (Kak and Slaney, 1988) provides equalities between Eqs. (2) and (3):

$$f(\omega,\ \theta)=F_V(\omega,\ \theta) \tag{4}$$

Substituting Eq. (4) into Eq. (3) and taking the inverse Fourier transformation, the spatially resolved volume fraction is expressed as

$$f(x,\ y)=\frac{1}{4\pi^2}\int_0^{\pi}d\theta\int_{-\infty}^{\infty}f(\omega,\ \theta)\exp[i\omega(x\cos\theta+y\sin\theta)\,|\,\omega\,|\,d\omega] \tag{5}$$

Let $P(r,\ \theta)$ be equal to the inner integral and define a function that satisfies

$$\phi=|\,\omega\,| \tag{6}$$

then from convolution Eg. (7) is derived.

$$\begin{aligned}P(r,\ \theta)&=\frac{1}{2\pi}\int_{-\infty}^{\infty}f(\omega,\ \theta)\,\phi(\omega)\,e^{i\omega r}d\omega\\&=\int_{-\infty}^{\infty}f(r,\ \tau)\,\phi(r-\tau)\,d\tau\end{aligned} \tag{7}$$

Substituting Eq. (7) into Eq. (5) gives

$$f(x,\ y)=\frac{1}{2\pi}\int_0^{\pi}d\theta\int_{-\infty}^{\infty}f(\tau,\ \theta)\,\phi(x\cos\theta+y\sin\theta-\tau)\,d\tau \tag{8}$$

Since $f(r,\ \theta)$ is known only at discrete measurement points, it is necessary to convert the integral form of Eq. (8) into a discrete summation approximation as

$$f(x,\ y)=\frac{1}{MN}\sum_{j=1}^{N}\sum_{k=1}^{M}f(r_k,\ \theta_j)\,\phi(x\cos\theta_j+y\sin\theta_j-r_k) \tag{9}$$

where $r_k=-1+2k/M$ and $\theta_j=(j-1)\,\pi/N$. M and N represent the number of scanning and the number of projection angles, respectively. The inverse Fourier transformation of Eq. (6) can provide a choice of the filter function $\phi(r)$. If l is the distance between $(r_k,\ \theta_j)$ and $(x,\ y)$, the value of $\phi(l)$ in Eq. (9) indicates the effectiveness of $f(r_k,\ \theta_j)$ on $f(x,\ y)$, which is the weighting factor. When a distribution in space resembles a Gaussian distribution, a Shepp and Logan filter function (Shepp and Logan, 1974) is commonly used, which is

$$\phi(0)=\frac{M^2}{\pi} \tag{10}$$

$$\phi(r_k)=\frac{M^2}{\pi}(4k^2-1)^{-1},\quad k=1,\ 2,\ 3,\ \cdots \tag{11}$$

where l lies between r_k and r_{k+1} and $\phi(l)$ is linearly interpolated.

The local volume fraction from the LDPA can be calculated by applying the same method as that of the direct sampling cells.

4. Coordinate Corrected Interpolation of Measured Data

In order to improve the signal-to-noise level in the reconstructed data, a so-called 'coordinate corrected interpolation' (Lee and Chung, 1997) has been carried out from the actually measured projections such that the number of projections

can be effectively increased.

Figure 5 shows the sampling rate of the spray on different projection planes located at z=90 mm without air shrouding with N=12 and M=35. Measured data contours at 12 projection angles are shown. The twin sprays are aligned perpendicular to the 0 degree projection line such that the two-peak sampling rate is imaged along the r-coordinate for θ=0 or 180 degree. For the 90 degree projection the sprays are parallel to the projection line and a single peak-looking profile is imaged. As θ further increases, two-peak images are recovered.

The accuracy of the tomographic reconstruction with changing the number of scanning M and the number of projection angles N was investigated by Lee and Chung (1997). The measured data resolution with M=35 and N=12 is expanded to N=48 and M=69 by the interpolation as shown in Fig. 6, which is enough for

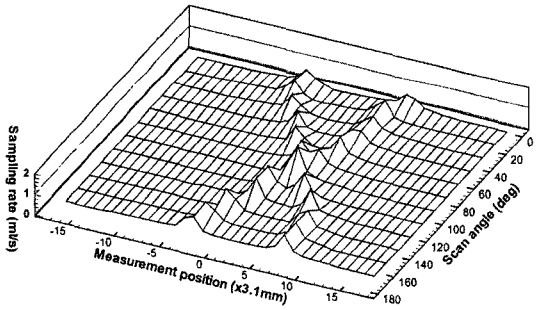

Fig. 5 Profiles of line-of-sight integrated injection rate without air shroud from effective 12 equiangular projections

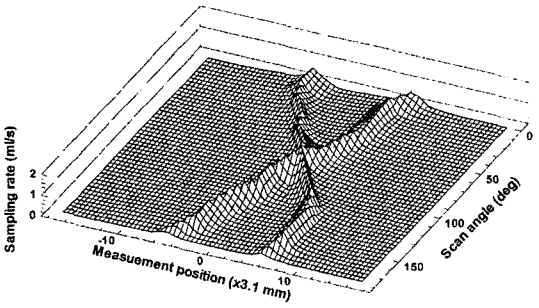

Fig. 6 Profiles of line-of-sight integrated injection rate without air shroud from effective 48 equiangular projections using interpolation

accurate tomogrpahic reconstruction. This data set has 48-equivalent projection angles. The interpolated data contours show significantly improved smoothness and continuity compared with the raw (noninterpolated) data variations in Fig. 5.

As the number of projections effectively increases by four times using the data interpolation, wavy noise generated from the tomographic reconstruction is almost effectively eliminated. Therefore, all the present reconstructions have been carried out after measured data are properly interpolated.

5. Results and Discussion

The local sampling rate from the line-of-sight data of the direct sampling cells cannot be compared directly with the local volume fraction from that of the LDPA; thus, the local sampling rate should be converted to local volume fraction. The LDPA system used in the present experiment received all diffraction patterns from drops in the measurement volume for 10 microseconds. Therefore, the local flow rate tomographically reconstructed from the data with direct sampling cells must be multiplied by 10 microseconds and divided by unit volume, which results in the volume in unit space, i.e. volume fraction.

The conversion equation for calculating the local volume fraction $F(x, y)$ from the local flow rate $f(x, y)$ is as follows:

$$F(x, y) = C_f f(x, y) \times \frac{t_s}{V_u} \tag{13}$$

where C_f, t_s and V_u are the coefficient of conversion, the LDPA's collecting time of diffraction signal from sprays and unit volume of direct sampling cells (27 mm^3), respectively. C_f is determined to match the peak value of the LDPA reconstructed volume fraction with that of the direct sampling cells. The value C_f obtained in this comparative study is 2.3. If the exact value of t_s is provided, the coefficient of conversion is expected to be near to 1. The exact t_s value can be suggested from the LDPA manufacturer. These results show that the local volume fraction which

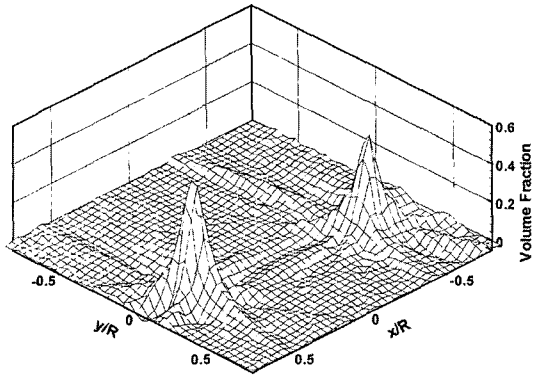

Fig. 7 Profiles of spatially resolved volume fraction without air shroud from effective 48 equiangular projections using interpolation (Direct sampling cell)

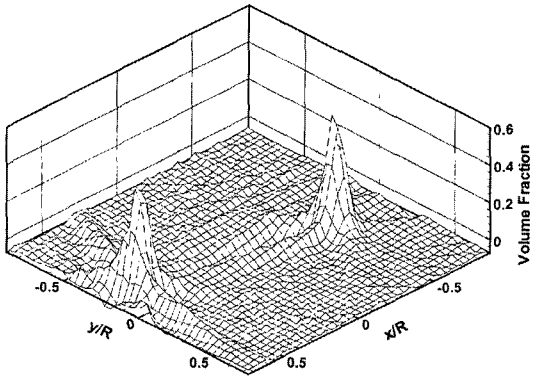

Fig. 8 Profiles of volume fraction without air shroud from effective 48 equiangular projections using interpolation (LDPA)

is obtained independent of the beam scattering length is reasonably accurate.

The reconstructed local sample rate from the interpolation shown in Fig. 6 is transformed to the local volume fraction using Eq. (13) and the results are shown in Fig. 7. Since the spray without air shroud should not develop any noticeable amount of drops or volume fractions in the region between the two sprays, the apparent wavy pattern does not have any physical representation but reflects mathematical noise due to an insufficient number of projections.

The peak values of the volume fraction are expected to be larger than those of the line-of-sight values since the line-of-sight values are integrated over a line-of-sight volume.

In the region between the peaks, the volume fraction maintains very low values. The noise level is much reduced compared to the results from the noninterpolated reconstruction, such that meaningful interpretation can be made (Lee and Chung, 1997).

The reconstructed volume fractions from the LDPA are shown in Fig. 8 for the injector without shroud air pressure. The results show similar local distributions of the volume fraction to those from the direct sampling.

Another reconstructed volume fraction from the direct sampling is shown in Fig. 9 for the injector with shroud air pressure of 0.03 MPa.

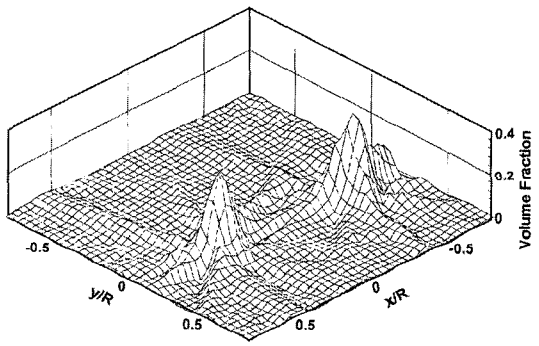

Fig. 9 Profiles of volume fraction with air shroud from effective 48 equiangular projections using interpolation (Direct sampling cell)

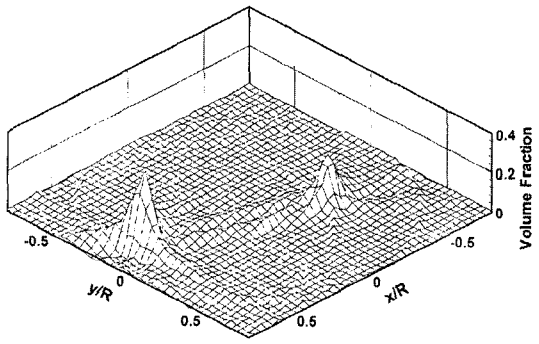

Fig. 10 Profiles of volume fraction with air shroud from effective 48 equiangular projections using interpolation (LDPA)

The reconstructed volume fraction from the LDPA is shown in Fig. 10 for the injector with shroud air pressure of 0.03 MPa. There is a little

discrepancy between the direct sampling cell and the LDPA methods. The needle of the injector used in the present experiment is steadily lifted approximately 2~5 minutes for each projection angle, which causes the solenoid performance of the injector to deteriorate and decrease the flow rate. The small discrepancy of the local volume fraction between the LDPA and the direct sampling may be due to the deterioration of the solenoid performance in the injector.

These results show that the reconstructed volume fraction from the LDPA can be used to calculate the local volume fraction of sprays tested without the standard spray vessel.

6. Concluding Remarks

The local volume fraction of twin-hole sprays from the line-of-sight data of the direct sampling cells was compared to estimate that from the line sight data of the LDPA by using tomographic reconstruction. The conversion coefficient C_f between the LDPA's and the direct sampling cell's volume fractions is obtained from the comparative study and the C_f value is 2.3 for the LDPA system. The LDPA's exact collecting time of diffraction signals from sprays, which is provided by the LDPA mannfacturer, could enhance the accuracy of the method.

This comparative study shows that the volume fraction from the line-of-sight data of the LDPA can be calculated exactly using tomographic reconstruction without the standard vessel which has a beam scattering length L_b.

References

Cha, S. S. and Sun, H., 1990, "Tomography for Reconstructing Continuous Fields from ill-Posed Multidirectional Interferometric Data," *Applied Optics*, Vol. 29, No. 2, pp. 251~258.

Cha, D. J. and Cha, S. S., 1996, "Holographic Interferometric Tomography for Limited Data Reconstruction," *AIAA Journal*, Vol. 34, No. 5, pp. 1019~1026.

Cormack, A. M., 1963, "Representation of a Function by its Line Integrals, with Some Radiological Applications," *J. Appl. Phys.*, Vol. 34, pp. 2722~2727.

Cormack, A. M., 1973, "Reconstruction of Densities from Their Projections with Application in Radiology Physics," *J. Phys. Assoc.*, Vol. 6, pp. 361~369.

Dodge, L. G., Rhodes, D. J. and Reitz, R. D., 1987, "Drop-size Measurement Techniques for Sprays : Comparison of Malvern Laser-Diffraction and Aerometrics Phase/Doppler," *Applied Optics*, Vol. 26, No. 11, pp. 2144~2154.

Eckbreath, A. C., 1987, *Laser Diagnostics for Combustion Temperature and Species*, pp. 362~401.

Gordon, R. G., Herman, G. T. and Johnson, S. A., 1975, "Imaging Reconstruction from Projections," *Sci. Am.*, Vol. 233, pp. 56~68.

Goulard, R. and Emmerman, P. J., 1980, "Combustion Diagnostics by Multianular Scanning," *Inverse Scattering Problems in Optics*, Springer Verlag, Berlin, pp. 215~235.

Jeong, S. J. and Lee, S. Y., 1992, "Experimental Study on the Flow Characteristics of a Confined Spray," *Transactions of KSME*, Vol. 16, No. 5, pp. 1011~1018.

Kak, A. C. and Slaney, M., 1988, *Principles of Computerized Tomographic Imaging*, IEEE Press, New York.

Lee, C. H. and Chung, S. H., 1997, "Tomographic Reconstruction of Asymmetric Spays from a Twin-Hole Air Shroud Injector," *Atomization and Sprays*, Vol. 7, No. 1, pp. 184~197.

Malvern Instruments Ltd., 1991, *Malvern System*, 2600 Instruction Manual.

Rowely, P. D., 1969, "Quantitative Interpretation of Three-Dimesional Weakly Refractive Phase Objects Using Holographic Interfermetry," *J. Opt. Soc. Am.*, Vol. 59, p. 1496.

Santro, R. J, Semerjian, H. G., Emmerman, P. J. and Goulard, R., 1981, "Optical Tomography for flow Field Diagnostics," *International Journal of Heat and Mass Transfer*, Vol. 24, No. 7, pp. 1139~1150.

Shepp, L. A. and Logan, B. F., 1974, "Reconstructing Interior Head Tissue from X-ray Transmissions," *IEEE Trans.*, Vol. NS-21, pp. 228~236.

Slepicka, J. S. and Cha, S. S., 1997, "Three Dimensional flow Diagnostics by Holographic Diffraction Image Velocimetry," *Proceedings of optical technology in fluid, thermal, and combustion flow III, SPIE-The International Society for Optical Engineering*, Vol. 3172, pp. 2226~232.

Swenny, D. W. and Vest, C. M., 1973, "Reconstruction of Three Dimensional Refractive Index Fields from Multidirectional Interferometric Data," *Applied Optics*, Vol. 12, pp. 2649~2664.

Yang, S. Y., Lee, C. H., Koo, J. A. and Chung, S. H., 1999, "An Experimental Study of Reconstruction from Laser Diffraction Measurement for Axisymmetric Sprays," *Transactions of the Korean Society of Automotive Engineers*, Vol. 8, No. 1, pp. 10~16.

Yule, A. J., Ah Seng, C., Felton, P. G., Ungot, A. and Chigier, N. A., 1981, "A Laser Tomographic Investigation of Liquid Fuel Sprays," *Proc. Combust. Inst. The Combustion Institute*, Vol. 18, pp. 1501~1510.

Zhu, H. M., Sun, T. Y. and Chigier, N., 1987, "Tomographic Transformation of Malvern Spray Measurements," *Atomization and Sprays*, Vol. 3, pp. 89~105.